The Widening Process of Straight Stream Channels in Alluvial Rivers

By Yuichiro FUJITA and Yoshio MURAMOTO

(Manuscript received March 31, 1982)

Abstract

The widening process of straight stream channels is the most fundamental and simple fluvial process in alluvial rivers, though it is hardly observed in natural rivers. Prediction of this process based on the hydraulic consideration is a first step for the elucidation of more complicated fluvial processes in alluvium which relate to extreme river disasters.

In this paper, as for the straight channel widening, the movement path of the sand eroded from a side bank and the lateral sediment transport are clarified by tracer tests and changes with time of cross sectional shape in detailed experiments, and by using these results the process of cross sectional variation is simulated under longitudinally uniform condition and problems in the analysis are pointed out.

In addition, the widening process under longitudinally varying conditions are dealt with by a extended one-dimensional analysis with the consideration of the initial and the boundary condtions. The applicability of this analysis proves to be high till the beginning of channel meandering mainly caused by well-developed alternating bars, though the analysis has two major points to be improved. One of these points is to find out the equation of the side bank erosion expressing the actual process including the conditions of bank collapse and effects of bed and water level variations, and the other is to give the upstream boundary conditions suitably for the case when an initial ability of sediment transport of the stream channel differs largely from the rate of sand supplying.

1. Introduction

In self-formed rivers, long straight reaches are seldom noticed. The channel widening of a straight stream is presumed to occur in rectilinear river course excavated artificially such as a cutoff chute or a flood control channel. However, in some countries where a great population is concentrated along river courses, as in Japan, even the stream channels newly cut are usually protected immediately by revetments or riprap works, hence the channel widening phenomenon is hardly observed in alluvial rivers. But, the channel widening phenomenon is the simplest and the most fundamental process of stream channel variation, and appears in the early stages of fluvial processes which arise from the straight stream channels. At those stages, sand bars, especially alternating bars, are not formed or their wave height has not developed sufficiently to lower their migration velocity. Hydraulic conditions of the stream channel during this widening process govern the development of the bars

and subsequent stream channel patterns. The elucidation of the widening process of a straight channel is, therefore, regarded as one of the basis to clarify the mechanisms of more complicated fluvial processes occuring in alluvial rivers.

The plane variation of stream channel can be perceived, in general, as a river bed variation controlled by a change of sediment transport in both longitudinal and transverse directions under influent and effluent conditions of sediment at both the upstream and the downstream ends of the object reach and at the water's edges along both the side banks. The difficulties in approaches to the plane variation of stream channel, as well as in a plane analysis of the flow characteristics, are that boundaries setting limits to the flow field change with time, even in the case of the straight channel widening. However, in this case, the relation of sediment continuity is rather easily rearranged being divided into two parts, one of which is the sediment eroded from both the side banks and carried to the bed; and the other is the bed variation due to a longitudinal fluctuation of sediment load and to the sediment supplied from the side banks. Studies on the straight channel widening as above-mentioned have been mainly developed in our country, and the outline of these studies is as follows.

Hasegawa-Kudo-Yamaoka[1] induced an equation predicting stream width change with time in the process of uniform channel widening in longitudinal direction on the consideration of the sediment transport and its continuity on the side bank slope, assuming that cross sectional area of stream flow is constant with time. However, their approach had an inadequate assumption in it that some variable quantities were regarded as constants and had some severe limitations for the execution of its analysis. Adachi-Nakato[2] introduced a term relating to the channel widening into the continuity equation of sediment and rearranged them into a diffusion equation of channel bed variation, supposing the locally uniform flow and neglecting the influence of the sand eroded from side bank on the bed variation on the basis of a order estimation of their experimental results. They pointed out the necessity to clarify the mechanism of channel widening process for the solution of the equation above. As for this mechanism, Tsubaki-Hirano-Tanaka[3] reduced a bed load function on the side bank slope based on the consideration of a balance of forces acting on a sand particle on the slope. Introducing this function into the continuity equation of sediment, and assuming a similarity of channel cross sectional shape they presented equations governing the stream channel widening. Though the results of their analysis in case of the uniform widening showed a good agreement with experimental values, the similarity hypotheses of cross sectional shape was more or less inadequate and manipulation of the continuity equation of sediment lacked clarity to some extent. On the other hand, Ashida-Muramoto-Narai[4] considered the balance of sediment and cleared up its continuity relation by dividing it into the rate of bed variation and that of side bank erosion. They applied the one-dimensional analysis of channel bed variation to the process of the channel widening, that is, they regarded the term relating to the channel widening included in the continuity equation of sediment, which is shown by Adachi et al.[2], as influent sediment from the

stream sides, and defined the relation between this sand supplying rate and hydraulic quantities as the function of side bank erosion rate to complete the equations concerned with the analysis of channel variation. In addition, they postulated the function of side bank erosion rate similar to the bed load function of Brown type on the dimensional consideration and compared the results of the analysis with a few experiments. Similarly, Hirano[5], rearranging the continuity relation in the study by Tsubaki et al.[3], turned the bed load function on the side slope into the function of side bank erosion rate, and analyezd the channel widening process. Furthermore, Muramoto-Tanaka-Fujita[6] modified the side erosion function by the shear distribution and executed the analysis under the various stream channel conditions to clarify the validity and the limit of the analysis. Recently, Hasegawa[7] has clarified the uniform widening process in longituidnal direction of a straight channel on considering sediment transport in non-equilibrium state on the side bank slope in detail. His approach is very excellent, but it is rather complicated and seems difficult to apply to the prediction of the fluvial process, even in the straight channel though he has shown some examples of the application.

Thus, it has become fairly general to predict the widening process of straight stream channel by the extended one-dimensional analysis of stream bed variation. In this paper, fundamental characteristics of the variation process of a straight channel are considerd by means of detailed experments on the viewpoint of sediment movement from the side banks to the stream bed and the validity of the extended one-dimensional analysis is confirmed by the applications to the widening processes under various hydraulic conditions.

2. Experiments on the widening process of a straight channel

2.1 Experimental procedure

Experiments were carried out in a 8 m-long reach of a concrete flume of 1.24 m in width, 0.55 m in depth and 12 m in length, by using a rather uniform sand, the
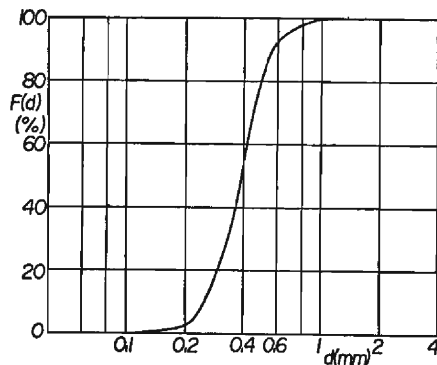

Fig. 1 The grain size accumulation curve of the sand used.

mean and median diameters of which were $d_m=0.42$ mm and $d_{50}=0.39$ mm respectively (**Fig. 1**).   Initial stream channel was formed in a straight ditch with prescribed cross sectional shape and slope by a blade attached to a grader which is handled along the slope lines drawn on the both side walls.   The stream bed of the downstream end was fixed at a constant height by a sill and the sediment washed out was trapped on the downstream flume bed from the sill.   At the upstream end of the experimental reach, the sand was supplied at a arbitrary rate by a screw type of sand feeder.   Flow discharge was controlled by valve operation and measured by a trapezoidal weir at the inlet.

In every experiment, the bed profile and the sediment washed out from the sill were measured, breaking the flow at suitable time intervals according to the channel process, while water surface level and stream width were measured by a point gauge just before the flow break.   Furthermore, pictures of the plane forms of the streams were taken at rather short time intervals to record the channel variation.   The cross sectional shapes of stream channel were measured precisely and tracer tests of sand particles colored on the side slope were carried out by photographing and sampling. In Run T-5, the sand on the bank slope was replaced with the colored sand at 3.0 to 3.02 m downstream reach from the inlet and the sand particles were traced.   The dispersion ranges of colored particles were measured at two flow breaks of 20-minute intervals.   At the last flow break sand particles on the bed were picked at denser spacing near the replacing point by a core-sampler of 6 mm diameter from the bed surface to the depth of 3 to 5 cm corresponding to bed forms.

The experimental conditions are shown in **Table 1.**   Initial cross section of the stream channel were trapezoidal in shape, top width, bottom width and height of which were 35 cm, 25 cm and 5 cm respectively except for Run T-5.   In the runs of

Table 1   The experimental conditions.

Run No.	Initial cross section			Initial bed slope	Discharge (l/s)	Sand supplying rate (cm/s)	Flow duration (hr:min)
	Bottom width (cm)	Side slope	Bank height (cm)				
S-1				1/100		2.0	3 : 02
2						0	19 : 33
3	25	1 : 1	5	1/200	1.6	1.5	9 : 07
4							10 : 03
5				1/100		0	10 : 00
6							4 : 00
T-1					1.0	0.88	0 : 17.5
2	25	1 : 1	5	1/200		1.53	0 : 55
3					3.0	2.13	1 : 50
4				1/100		3.65	2 : 01
5	55	55	5	1/200		0	0 : 40

S series the discharge was fixed at 1.6 l/sec to compare various fluvial processes due to the difference of the sediment supply and the initial bed slope.

2.2   Outline of experimental results

At the early stage in every experiment, the whole stream channel bed was covered with standing waves of about 5 cm wave length and the stream channel was widened uniformly in longitudinal direction to raise the bed.   However, after this stage the channel widening processes differed from each other according to the sand supplying conditions.   When the sand was not fed at the inlet, bed degradation was propagated from the upstream end, decreasing the channel widening rate to form a gradually expanding channel in the upstream reach.   At the same time, conspicuous sand ripples with the wave length of 10 to 20 cm and the wave height of 1 to 2 cm appeared from the upstream reach and scoured the side bank intermittently concentrating the flow against the bank locally.   On the other hand, in cases of sand supplying the bed where sand ripples did not occur always had a tendency to aggrade and the channel was widened rapidly and rather uniformly.   In the runs of S-series, the plane forms of the stream channels remained straight and no meandering bend was observed, though faint flow meanderings were noticed if channel width became more than 60 cm no matter whether sand was supplied or not.

Longitudinal variations of mean hydraulic quantities at each cross section corresponded to those of the channel width; they were small in cases of sand supplying while rather large in cases without sand supplying.   But even in the latter cases ranges of the variation rate were within 20% of the averaged values in the whole experimental reach.   Flow resistance in the experiments was large, especially in the cases of no sand feeding: the flow velocity coefficient U/U_* was 6 to 8 reflecting the large form drag due to the remarkable ripples.   The sediment discharge both total and per unit width measured at the downstream end showed a diminishing trend with time in all runs and agreed with that predicted by bed load formulae that bed load decrease in widening straight channel if a bed slope keeps a constant value.   The measured values of sediment load were small in the cases of no sand supplying because of the form drag of the sand ripples, but they seemed to be included within the range of previous experimental values, because they agreed well with calculated values from Ashida-Michiue's bed load formula[8].

2.3   Traveling path of the sand particles from the side bank

The erosion process of stream channel banks includes two cases.   One of them is the case that the erosion of side slope is accompanied with intermittent collapse of the bank above the water surface and the other is the csae that continuous deformation of the side bank is caused only by sliding and rolling of sand particles on the side slope.   In Run T-5 where tracer test of sand grains were tried, small scale collapse of a side bank happened at the replacement point with colored sand and immediately after this collapse almost all the collapsed sand was covered with a ripple.

Fig. 2 shows the dispersion ranges of the colored sand on the bed.   Curves A and B depict those on the bed surface at 20 minutes and at 40 minutes after the beginning respectively, while Curve C describes the existing limit of the colored sand picked up by the sampler.   The origin in **Fig. 2** is the foot point of the colored sand located at 1.5 cm from the water's edge and 0.9 cm below the water surface. The x-axis is taken downstream-ward and the y-axis is taken from the water's edge to the centerline of the stream channel.   The region where curve B is closer to the water's edge than curve C is where the collapsed sand was covered with the ripple and curve B in this region almost shows the plane form of this ripple.   It can be pointed out from **Fig. 2** that the collapsed sand was transported 10 cm away from the foot of the bank, and at $y > 10$ cm gradients of these curves become a nearly constant value showing an approximately identical direction of sand transport regardless of bank collapse and that a part of side bank sand could reach the center of the channel of 60 cm width after a longitudinal traveling of 1 m.
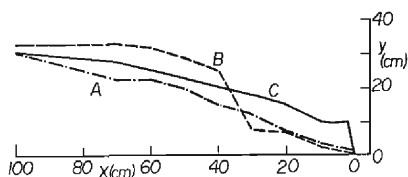

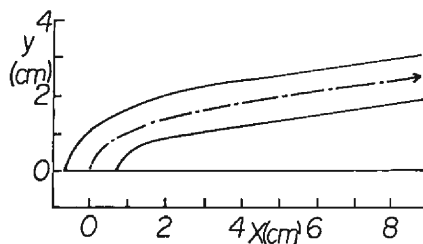Fig. 2   The dispersion ranges of the colored sand.

Fig. 3   The dispersion range of the colored sand by photographing.

Next, by the result of photographing in Run T-3, an existing range of the colored sand near the bank is shown in **Fig. 3**.   The direction of the colored sand motion has a deviation angle of 10° to 15° at 2 cm away from the water's edge but this angle decreases to less than several degrees at $y > 3$ cm.   This change of the direction is very similar to that of curve A in **Fig. 2** in spite of a considerable difference of hydraulic conditions.

Finally, a plane distribution of the colored sand is demonstrated in **Fig. 4** with contour lines or histograms of sand grain numbers sampled in a column of 6 mm-diameter.   Though the sampled sand includes both the sand collapsed down on the bed and that eroded continuously, they are not separated in **Fig. 4**.   Upstream one of two peaks of the grain distribution recognized in an $x = 0–40$ cm reach was a peak of the collapsed sand preserved by the ripple cover aforementioned and the other seemed to be formed through the promotion of the bank erosion and its transport due to the water concentration caused by the ripple.   Therefore, the traveling velocity of the latter peak 30 cm/13 min $= 0.04$ cm/sec represents the migration rate of this ripple, which agrees well with that presumed from the bed load at the downstream end and the wave height of this ripple.   Thus, even the bed cofiguration of micro scale affects on the local bank erosion if it develops prominently near the bank.
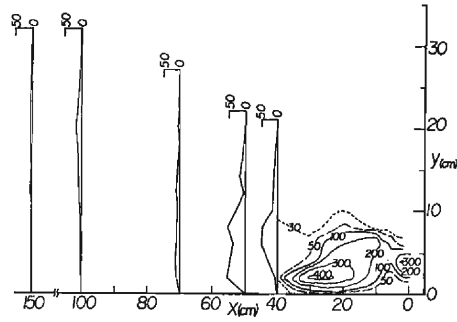
Fig. 4 The plane distribution of the colored sand.

The sand eroded from the side banks was carried along the path above-mentioned to contribute to the stream bed variation. This contribution may be made clearer by evaluating the sediment balance between the side banks and the channel bed rather than by the tracer test. Especially, sediment transport in the transverse direction can be estimated in case that hydraulic conditions change little in longitudinal direction.

2.4 Variation of cross sectional shape and sediment balance

Variation of cross sectional shape at $x=2$ m and 3 m stations (3 and 4 m downstream from the inlet respectively) in Run T-4 are shown in **Fig. 5** as an example. Though the development of ripples were suppressed considerably, fluctuations of the
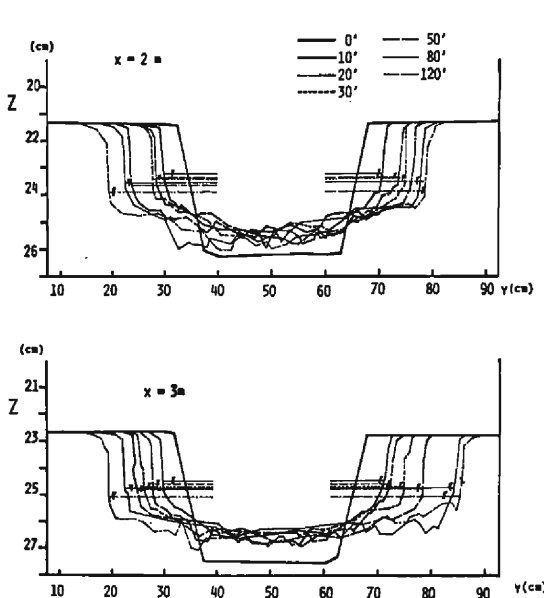

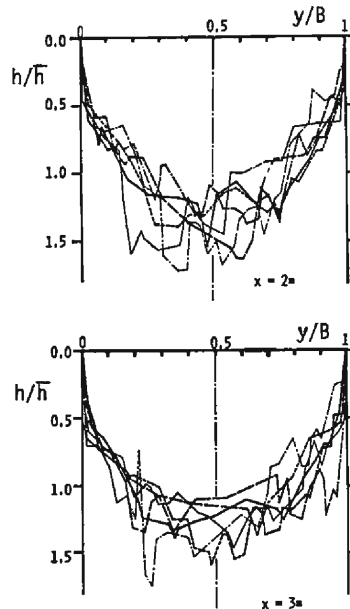Fig. 5 The variation of the cross sectional shape.

Fig. 6 The variation of the normalized cross sectional shape.

bed appearing in these figures were inevitable because the grain diameter of the sand used was small and bed configuration of micro scale is formed easily.   In every cross section, remarkable bed aggradation and bank erosion occurred at the early stage and bank erosion continued till the end of the experiment while mean bed elevation seemed to become constant even though local variation were fairly large, which might be ascribed to a restraint of the boundary conditions of the constant bed elevation at the downstream end and the scarcity of sand supplied at the inlet because the length of experimental reach was 8 m and regarded to be short enough for the boundary conditions to be propagated in the whole reach rapidly.

Similarity of the cross sectional shape is examined in **Fig. 6**, normalizing the transverse distance and the vertical length with the channel width and the mean flow depth respectivley.   Actual difference among the cross sectional shapes is dif- ficult to grasp because the area of each shape is also normalized to unity and the fluctuations of the bed are apt to be amplified in case of small flow depth in parti- cular.   However, in **Fig. 6** the cross sectional shape at $x=2$ m upstream side is close to a triangular shape while that at $x=3$ m downstream side is rather rectangular, hence the assumption of the similarity in cross sectional shapes of straight stream channels does not seem to be valid.

Meanwhile, **Fig. 7** shows the volume of cross sectional change, letting the erosion positive.   The volume change during the early stage is large in every section, as aforementioned, and the changes of the bed largely diminish after this.   Accumulat- ing this volume from both side banks to the center of the stream channel, the results are shown in **Fig. 8**.   The sum of two accumulated values at the center represents the variation rate of total sediment transport in longitudinal direction, where its posi- tive vlaue means the increasing tendency of sediment transport.   If the stream channel varies uniformly in longitudinal direction, both the two curves coincide to zero at the center and at the same time these curves express the distribution of the trans- verse sediment transport.   In **Fig. 8**, since these curves during $T=0'-10'$ coincide to
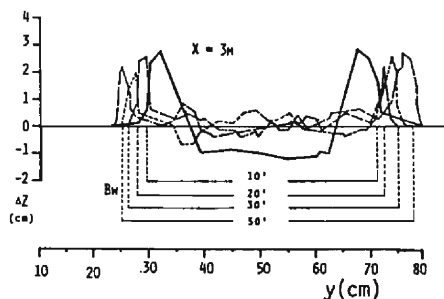

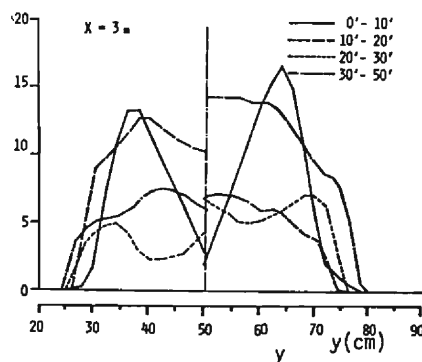Fig. 7   The volume of cross sectional change.

Fig. 8   The accumulated volume of cross sectional change.

nearly zero at the center, it can be judged that uniform channel widening process occurred in this reach at the early stage of the experiment. Accordingly, mean transverse sediment load per unit longitudinal length q_{By} can be computed for this time duration, and if the longitudinal sediment transport rate is estimated at each point on the bed by use of a bed load formula, the direction of sediment movement can be calculated as follows:

The longitudinal bed load per unit width, q_{By}, is assumed to be expressed by the Brown type function in which the critical tractive force is taken into account,

$$q_{Bx*} = q_{Bx}/U_* d_m = M_1 \tau_* (1 - \tau_{*c}/\tau_*)^m \quad \cdots\cdots\cdots\cdots\cdots\cdots\cdots\cdots (1)$$

and for the sake of simplicity, distribution of the nondimensional tractive force τ_* and the critical one τ_{*c} are calculated from

$$\tau_* = U_*^2/(\sigma/\rho - 1)g d_m = (H-Z)I_e \cos\theta/(\sigma/\rho - 1)d_m \quad \cdots\cdots\cdots\cdots (2)$$

$$\tau_{*c} = U_{*c}^2/(\sigma/\rho - 1)g d_m = \tau_{*cL} \cos\theta \sqrt{1 - \tan^2\theta/\tan^2\varphi} \quad \cdots\cdots\cdots\cdots (3)$$

where M_1 and m are experimental constants, U_* is the shear velocity, U_{*c} is the critical one, g is the acceleration of gravity, H and Z are elevation of the water surface and the stream bed respectively, I_e is energy slope, θ is a transverse slope angle of the bed, φ is a static frictional angle of the sand, ρ and σ are the density of water and sand particles respectively, and suffix $_L$ denotes the values in case of the horizontal bed.
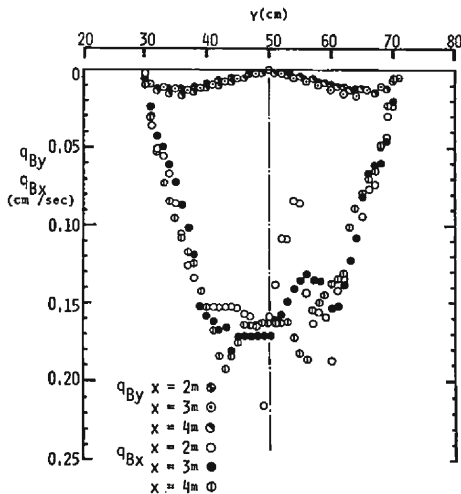
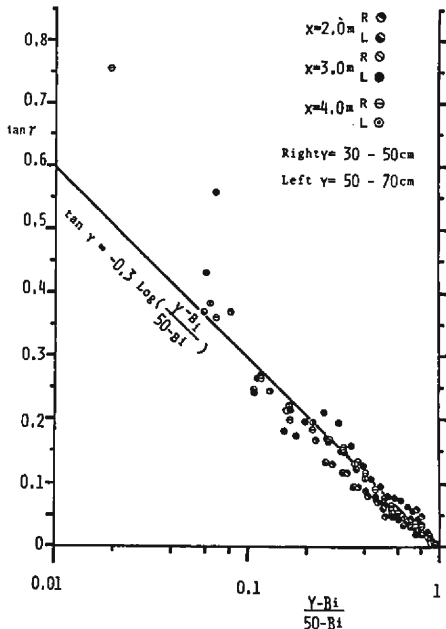Fig. 9　The distribution of q_{By} estimated from Fig. 8 and that of q_{Bx} by use of eqs. (1)–(3).

Fig. 10　The mean direction of sediment movement evaluated from Fig. 9.

Applying eqs. (1)–(3) to the cross sectional shape at $T=10'$ and putting $M_1=3$ and $m=1$ based on the results of bed load measurement at the donwstream end, q_{Bx} is computed, while q_{By} is determined from the curves in **Fig. 8**. The results are depicted in **Fig. 9**, in which the distribution of q_{Bx} is rather irregular reflecting the fluctuations of the bed. Neglecting this irregularity, however, the distribution of q_{Bx} is symetric as well as that of q_{By}. The mean direction of sediment movement, $\tan \gamma$, is computed dividing the values of q_{By} by those of q_{Bx}. The calculated values of $\tan \gamma$ are demonstrated in **Fig. 10** as a function of nondimensional lateral distance by a half width of the stream flow, $y'=(y-B_i)/(y_c-B_i)$, where B_i and y_c denote the positions of each water's edge and the center of the stream channel respectively. An empirical equation for $\tan \gamma$ is obtained as follows:

$$\tan \gamma = q_{By}/q_{Bx} = -0.3 \log (y-B_i)/(y_c-B_i) \quad \cdots\cdots\cdots\cdots\cdots\cdots\cdots (4)$$

in which the factor of 0.3 seems to change according to the process and the scale of experiments as well as to the other hydraulic conditions. But eq. (4) at least gives fairly good approximate values for the uniform widening process at early stages of the same scale experiments. The directions of mean particle paths in **Fig. 3** and **Fig. 4** are almost in the same range for $\tan \gamma$ as in **Fig. 9**.

2.5 Variation process of the cross section

In the longitudinally uniform widening process, as the sediment movement proves to be approximately expressed by eqs. (1)–(4), the variation of the cross sectional shape can be simulated, combining the following equations with the above ones.

The motion and the continuity equations of uniform flow and the hydraulic resistance formula are as follows:

$$I_e = \sin i = U_*{}^2/gR \cdots\cdots\cdots\cdots\cdots\cdots\cdots\cdots\cdots\cdots\cdots\cdots\cdots\cdots\cdots\cdots\cdots (5)$$
$$Q = UA = \text{const.} \quad \cdots\cdots\cdots\cdots\cdots\cdots\cdots\cdots\cdots\cdots\cdots\cdots\cdots\cdots\cdots (6)$$
$$U/U_* = c = \text{const.} \cdots\cdots\cdots\cdots\cdots\cdots\cdots\cdots\cdots\cdots\cdots\cdots\cdots\cdots\cdots (7)$$

The continuity of the stream bed is expressed by

$$(1-\lambda)\frac{\partial Z}{\partial t} + \frac{\partial q_{By}}{\partial y} = 0 \quad \cdots\cdots\cdots\cdots\cdots\cdots\cdots\cdots\cdots\cdots\cdots\cdots\cdots (8)$$

for uniform widening process in longitudinal direction, and from the geometrical condition as shown in Fig. 11,

$$\int_{B_1}^{B_2} (H-Z)dy = A \quad \cdots\cdots\cdots\cdots\cdots\cdots\cdots\cdots\cdots\cdots\cdots\cdots\cdots\cdots (9)$$
$$Z(B_1) = Z(B_2) = H \quad \cdots\cdots\cdots\cdots\cdots\cdots\cdots\cdots\cdots\cdots\cdots\cdots (10)$$
$$\cos \theta = 1/\sqrt{1+(\partial Z/\partial y)^2} \quad \cdots\cdots\cdots\cdots\cdots\cdots\cdots\cdots\cdots\cdots (11)$$
$$R = A\Big/\int_{B_1}^{B_2} \sqrt{1+(\partial Z/\partial y)^2}\, dy \quad \cdots\cdots\cdots\cdots\cdots\cdots\cdots\cdots (12)$$
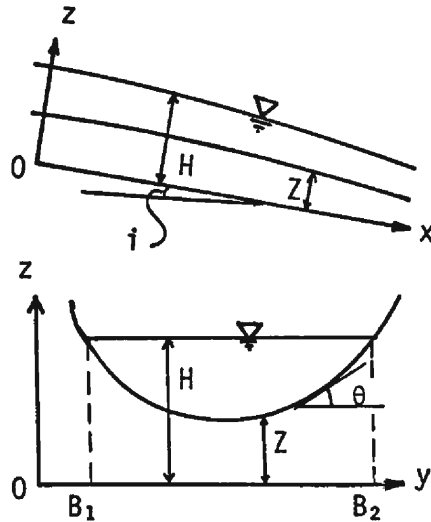
Fig. 11 A definition sketch of the coordinate system and notation.

are obtained, where Q is the discharge, A is the cross sectional area of flow, R is the hydraulic radius, $\sin i$ is the bed slope, λ is the porosity, t is the time of flow duration, U and c are the flow velocity and the velocity coefficient averaged in the cross sectional area respectively, and B_1 and B_2 are the positions of the water's edges.

These equations yield the following expressions nondimensionalized by the depth at the center H_1 and the stream width B_0 in the initial state.

$$\frac{\partial \zeta}{\partial t} = \frac{q_{B_0}}{2(1-\lambda)B_0 H} \{(\chi-\zeta)\cos\theta\}^{3/2}\left[\tan r \left(P+\frac{2}{1-r_0}\right)\cdot\right.$$
$$\left.\left\{\cos^2\theta\left(\frac{H_1}{B_0}\right)^2\frac{\partial^2\zeta}{\partial\eta^2}+\frac{1}{h-\zeta}\right\}\frac{\partial\zeta}{\partial\eta}-2P\frac{\partial}{\partial\eta}(\tan r)\right] \quad\cdots\cdots\cdots\cdots\cdots\cdots(13)$$

where

$$P = (1-r_0)/\{1-r_0(\chi-\zeta)\cos\theta\},$$
$$q_{B_0} = M_1 U_{*0}^3(1-r_0)/\{(\sigma/\rho-1)g\}, \quad r_0 = U_{*c}^2/U_{*0}^2,$$
$$U_{*0}^2 = gH_1\sin i, \quad \eta = y/B_0, \quad \zeta = Z/H_1, \quad \chi = H/H_1.$$

The process of the change in cross sectional shape was analyzed numerically by using this equation with the other relations for half of the cross section assuming the form to be symmetric. Boundary conditions required to execute the analysis are, at the water's edge,

$$\theta = \varphi \quad \text{and} \quad \partial q_{B_y}/\partial y = 0\cdots\cdots\cdots\cdots\cdots\cdots\cdots\cdots\cdots\cdots\cdots\cdots\cdots\cdots\cdots(14)$$

and at the center of the stream channel,

$$\theta = 0 \quad \text{and} \quad q_{By} = 0 \quad \cdots\cdots\cdots\cdots\cdots\cdots\cdots\cdots\cdots\cdots\cdots\cdots\cdots(15)$$

Besides, an amount of sand equal to the value of q_{By} calculated at the foot of the side bank is supposed to slide down from the side bank and to cause the receding of the water's edge. On the other hand, the initial and hydraulic conditions are decided from that of Run T-4, and the finite differences of y and t are $\Delta y = 0.25$ cm and $\Delta t = 0.5$ sec respectively, which are determined by trial and error because of the ambiguity of the stability and the convergence conditions. The analysis is carried out repeating the following procedure: the water surface level is calculated first to satisfy the eqs. (5)–(7) and (9)–(12) for the former cross sectional shape, and next a volume of the bed variation is computed during one time step by using the eqs. (1)–(4) and (13). In the calculation, if the bed slope happens to exceed the angle of repose of the sand, the bed is changed automatically to lower the slope to less than the angle of repose.

The result of the analysis is compared with the shape observed in **Fig. 12** and shows higher rates of the channel widening and the bed aggradation than those observed. But the shapes calculated fairly well resemble the observed one, and the method described above proves to be able to predict the variation process of channel cross section with considerable accuracy. For the improvement of the analysis it is necessary to make the boundary condition at the water's edge more valid and to modify the way the bed is dealt with in the case when the slope angle become larger than the static frictional angle or the angle of repose and when the collapse of a side bank occurs. Actually, the high rate of the widening is judged to be caused by the sand sliding on the side slope compelled automatically in the analytical procedure because the initial bank slope angle of 45° was larger than the angle of repose.

A similar analysis was carried out by Hasegawa[7] who used rather complicated equations on the basis of more detailed consideration of sediment movement including the bank collapse, but the mean hydraulic conditions such as mean shear stress and water surface level were determined by the interpolation of experimental values and therefore equations were not completed.

As mentioned above, the analysis of cross sectional variation of the stream channel is possible but in spite of the simplest conditions it is too complicated and therefore it is hard to apply to the cases under longitudinally varying conditions. In these
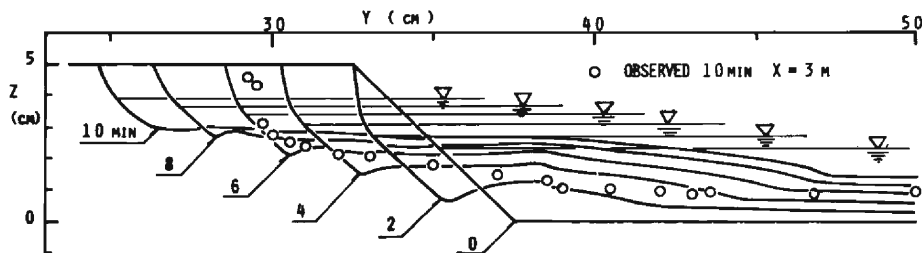

Fig. 12   The calculated change of a stream cross section.

cases, the one-dimensional analysis of stream channel variation has come to be applied fairly general, as stated in the introduction. The applicability of the one-dimensional anlaysis is considered for various experimental conditions in the next chapter, because the validity of this analysis has not been examined sufficiently yet.

3. The one-dimensional analysis of stream channel variation

3.1 Fundamental equations

Fundamental equations of one-dimension describing the widening process of straight stream channel are as follows. The cross sectional shape of the stream channel is regarded as wide and rectangular, and coordinate systems are taken according to the initial channel geometry, as shown in **Fig. 13**.

The continuity equation of the stream bed is, regarding the sand eroded from the side banks as the sand supply to the bed,

$$B(1-\lambda)\frac{\partial Z}{\partial t} + \frac{\partial Q_B}{\partial x} = q_s \quad \cdots\cdots\cdots\cdots\cdots\cdots\cdots\cdots\cdots\cdots\cdots\cdots\cdots\cdots\cdots(16)$$

while the relation of continuity of the side bank yields

$$q_s = (1-\lambda')(D-Z)\frac{\partial B}{\partial t} \quad \cdots\cdots\cdots\cdots\cdots\cdots\cdots\cdots\cdots\cdots\cdots\cdots\cdots(17)$$

where B is the stream width, Q_B is the total sediment load, q_s is the erosion rate of side banks per unit length, D is the elevation of top of side banks, and λ and λ' is the porosity of the stream bed and the side banks respectively.
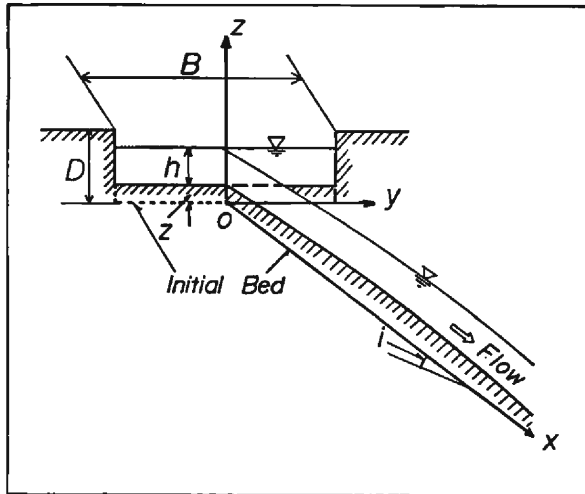

Fig. 13   A definition sketch of the coordinate system and the notation.

An equation the same as eq. (1) is used as a bed load function.

$$Q_B = Bq_B = BM_1\{(\sigma/\rho-1)g\}^{-m}d_m^{1-m}U_*(U_*^2-U_{*c}^2)^m \quad\cdots\cdots\cdots\cdots(18)$$

where q_B is bed load per unit width; d_m and U_{*c} are the mean diameter and the critical shear velocity of the bed material respectively; and U_* is the mean shear velocity on the bed.

As to the formula of side bank erosion, which has already been investigated in detail by the author[9] on the basis of hydrodynamic considerations, the next formula is used corresponding to the results in **2.4** for the sake of simplicity.

$$q_s = N_1(\sigma/\rho-1)g^{-m}d_m^{1-m}U_{*s}(U_{*s}^2-U_{*c}^2)^m \quad\cdots\cdots\cdots\cdots\cdots\cdots\cdots(19)$$

where N_1 is an experimental constant and U_{*s} is the mean shear velocity on the side bank slopes, which is expressed as $U_{*s}=\varepsilon U_*$ by using a constant ε relating to the shear distribution.

Assuming the locally uniform flow and the hydraulic resistance of the Chézy type

$$Q = UBh = \text{const.} \quad\cdots\cdots\cdots\cdots\cdots\cdots\cdots\cdots\cdots\cdots\cdots\cdots\cdots\cdots\cdots(20)$$

$$I_e = U_*^2/gh = I_0-\partial Z/\partial x \quad\cdots\cdots\cdots\cdots\cdots\cdots\cdots\cdots\cdots\cdots(21)$$

$$U/U_* = C=\text{const.} \quad\cdots\cdots\cdots\cdots\cdots\cdots\cdots\cdots\cdots\cdots\cdots\cdots\cdots(22)$$

where I_0 is the initial bed slope.

Substituting eqs. (18) and (19) for q_B and q_s into eqs. (16) and (17), and nondimensionalizing the dependent quantities by the initial values and the discharge, the equations above yield,

$$\frac{\partial \tilde{Z}}{\partial t} = K_0\tilde{B}^{-(2m+1)/3}\tilde{I}_e^{(2m-2)/3}(1-r_0\tilde{B}^{2/3}\tilde{I}_e^{-2/3})^{m-1}(2m+1-r_0\tilde{B}^{2/3}\tilde{I}_e^{-2/3})\cdot$$

$$\left\{\frac{\partial^2\tilde{Z}}{\partial x^2} - \frac{I_0}{D}\left(\frac{6m}{2m+1-r_0\tilde{B}^{2/3}\tilde{I}_e^{-2/3}}-2\right)\frac{\tilde{I}_e}{\tilde{B}}\frac{\partial \tilde{B}}{\partial x}\right\}+\alpha\frac{1-\tilde{Z}}{\tilde{B}}\frac{\partial \tilde{B}}{\partial t} \cdots\cdots\cdots(23)$$

$$\frac{\partial \tilde{B}}{\partial t} = P_0\frac{\tilde{B}^{-(2m+1)/3}\tilde{I}_e^{(2m+1)/3}}{1-\tilde{Z}}(\varepsilon^2-r_0\tilde{B}^{2/3}\tilde{I}_e^{-2/3})^m \quad\cdots\cdots\cdots\cdots\cdots(24)$$

$$\tilde{I}_e = 1-\frac{D}{I_0}\frac{\partial \tilde{Z}}{\partial x} \quad\cdots\cdots\cdots\cdots\cdots\cdots\cdots\cdots\cdots\cdots\cdots\cdots\cdots(25)$$

$$\tilde{h} = \tilde{B}^{-2/3}\tilde{I}_e^{2/3}\cdots\cdots\cdots\cdots\cdots\cdots\cdots\cdots\cdots\cdots\cdots\cdots\cdots\cdots\cdots\cdots(26)$$

where

$$K_0 = q_{B0}/3I_0(1-\lambda)(1-r_0)^m,$$

$$P_0 = q_{s0}/DB_0(1-\lambda')(\varepsilon^2-r)^m, \quad r_0 = U_{*c}^2/U_{*0}^2,$$

$$U_{*0} = (gQI_0/CB_0)^{1/3}, \quad \alpha = (1-\lambda')/(1-\lambda),$$

the suffix $_0$ indicates the initial values, and $\tilde{}$ denotes the non-dimensional quantites

such as $\tilde{Z}=Z/D$, $\tilde{B}=B/B_0$, $\tilde{I}_e=I_e/I_0$ and $\tilde{h}=h/D$.

The analysis is carried out numerically by using the following difference equations instead of eqs. (23)–(25) in which the term concerning $(\partial B/\partial x)$ in eq. (23) is neglected,

$$\tilde{Z}_{i+1,j} = \tilde{Z}_{i,j}+K_0\frac{\varDelta t}{(\varDelta x)^2}\tilde{B}_{j,j}^{-(2m+1)/3}\tilde{I}_{ei,j}^{(2m-2)/3}(1-\gamma_0\tilde{B}_{i,j}^{2/3}\tilde{I}_{ei,j}^{-2/3})^{m-1}$$
$$\times (2m+1-\gamma_0\tilde{B}_{i,j}^{2/3}\tilde{I}_{ei,j}^{-2/3})(\tilde{Z}_{i,j+1}-2\tilde{Z}_{i,j}+\tilde{Z}_{i,j-1})$$
$$+\alpha\frac{1-\tilde{Z}_{i,j}}{\tilde{B}_{i,j}}(\tilde{B}_{i+1,j}-\tilde{B}_{i,j}) \quad\cdots\cdots\cdots\cdots\cdots\cdots\cdots\cdots\cdots\cdots\cdots(27)$$

$$\tilde{B}_{i+1,j}-\tilde{B}_{i,j} = P_0\tilde{B}_{i,j}^{-(2m+1)/3}\tilde{I}_{ei,j}^{(2m+1)/3}(1-\tilde{Z}_{i,j})^{-1}$$
$$\times (\varepsilon^2-\gamma_0\tilde{B}_{i,j}^{2/3}\tilde{I}_{ei,j}^{-2/3})^m \quad\cdots\cdots\cdots\cdots\cdots\cdots\cdots(28)$$

$$\tilde{I}_{ei,j} = 1-(D/2\varDelta xI_0)(\tilde{Z}_{i,j+1}-\tilde{Z}_{i,j-1}) \quad\cdots\cdots\cdots\cdots\cdots(29)$$

where suffixes i and j denote the step numbers of time and distance respectively, and $\varDelta t$ and $\varDelta x$ are the finite differences, respectively.

3.2 Procedure of the analysis

The initial condition of bed profile is given by a non-dimensional function of x, $\tilde{Z}_0(x)$, by the initial bank height D of the channel in the experiment.

$$\tilde{Z}(x, t)\,|_{t=0} = \tilde{Z}_0(x) \quad\cdots\cdots\cdots\cdots\cdots\cdots\cdots\cdots\cdots\cdots\cdots\cdots\cdots\cdots(30)$$

On the other hand, the initial channel widths differ from each other by the discharge because of the trapezoidal cross section in these experiments. Therefore the initial condition is determined by eq. (31) in which h is substituted for the uniform flow depth computed from eq. (32) assuming $R=h$ even in the initial trapezoidal shape,

$$B_0 = B_W = B_D+2m_s h \quad\cdots\cdots\cdots\cdots\cdots\cdots\cdots\cdots\cdots\cdots\cdots\cdots\cdots(31)$$
$$C^2gI_0h(B_D+m_s h)^2=Q^2 \quad\cdots\cdots\cdots\cdots\cdots\cdots\cdots\cdots\cdots\cdots\cdots(32)$$

where B_D and m_s are the bottom width and the inverse slope of the initial trapezoidal shape of the channel cross section.

The boundary conditions must be given at two points of the upstream and the downstream ends. Since in all the experiments the bed elevation was fixed by a sill at the downstream end where $x=x_1$ the boundary condition is

$$\tilde{Z}(x, t)\,|_{x=x_1} = \text{const.} \quad\cdots\cdots\cdots\cdots\cdots\cdots\cdots\cdots\cdots\cdots\cdots\cdots(33)$$

Meanwhile, the boundary condition at the upstream end must correspond to the condition of the sand supply, hence it is given from a bed slope satisfying the relation that the bed load at the upstream end Q_{Bu} become equal to the rate of sand feeding Q_{BS} for the stream width at that time. This condition is obtained from eqs. (18) and (20)–(22) to be

$$\hat{I}_{eu} r_0^{-3/2} \left(1 - \frac{\sigma/\rho - 1}{M_1} \frac{C}{Q} \frac{Q_{BS}}{I_0} \hat{I}_{eu}^{-1} \right) = \tilde{B}_u \quad \cdots\cdots\cdots\cdots\cdots\cdots\cdots(34)$$

in nondimensional form for $m=1$ mentioned later, where suffix $_u$ represents the values at the upstream end. Accordingly, in the case of no sand supply ($Q_{BS}=0$) eq. (34) yields $\hat{I}_{eu} = \tilde{B}_u r_0^{3/2}$, that is a static equilibrium slope, and eq. (24) indicates $\tilde{B}_u = 1$, then

$$\hat{I}_u = \hat{I}_k = r_0^{-3/2} \quad \cdots\cdots\cdots\cdots\cdots\cdots\cdots\cdots\cdots\cdots\cdots\cdots\cdots\cdots\cdots\cdots(35)$$

is valid, where $\hat{I}_k$ is the ratio of the static equilibrium slope to the initial one.

The analysis is executed, repeating the computation of eqs. (28) and (29) based on the one step former channel geometry and the determination of the geometry at the next step by the substitution of its results into eq. (27)

Among the constants used in the equations, $m=1$, $\varepsilon=0.75$, $\lambda=0.4$ are fixed in all analyses. The value of m is selected because many usual functions of the bed load indicate a relation of $q_B \propto U_*^3$ for large tractive force. $\varepsilon=0.75$ is determined, referring to the computation of the shear distrbution in trapezoidal cross section by Lane[10] and this value agrees well with the results of the detailed consideration on the mechanism of side bank erosion[9]. The other constants are selected corresponding to hydraulic conditions of the experiments, which consist of two series of experiments. One of them is that of S series in this paper and the other is a series of large

Table 2 The experimental conditions in the large flume.

| Exp. No. | Cross Section of Channel (Trapezoidal shape) | | | Bed Slope | Stream Length (m) | Dis-charge (l/s) | Flow Duration (hr-min) | Notation |
	Bottom Width (cm)	Side Slope	Deph (cm)					
1-1 -2	100	1 : 1	20	1/200	130	7.5 15.0	100–00 30–29	
II	100	1 : 1	20	1/200	128	15.0	28–41	
III	50	1 : 2	10	1/200	120	6.0	71–26	
IV	50	1 : 2	10	1/200	110	15.0	25–00	
V U.R. D.R.	50	1 : 2	10	1/200 1/500	110	6.0	55–30	Two step slope
VI U.R. D.R.	50	1 : 2	10	1/200 1/500	100	15.0	37–30	
VII	50	1 : 2	10	1/200	110	6.0~30.0	31–00	Varying flow
VIII	25	1 : 2	5	1/200	110	5.0	22–00	
IX	50	1 : 2	10	1/200	110	15.0	30–00	Left side: loose Right side: rigid
X	100	1 : 2	20	1/200	42.3	20.0	17–21	
XI	50	1 : 2	10	1/200	42.8	15.0	12–07	Sand supply
XII	50	2 : 1	40	1/200	42.4	15.0	44–35	
XIII	50	1 : 1	20	1/200	42.8	15.0	15–40	

U.R.: Upstream Reach, D.R.: Downstream Reach

scale experiments carried out in Ujigawa Hydraulic Laboratory by using one of the largest flumes. These are listed in **Table 2**[11]. For these series the values of λ', M_1 and N_1 are changed, and the values of $\lambda'=0.4$, $M_1=3$ and $N_1=1.2$ are used in the analysis of S series, while those $\lambda'=0.45$, $M_1=10$ and $N_1=3$ are used for the latter series. The smaller values of M_1 and N_1 for S series reflect the decrease in effective tractive force due to the form drag of the sand ripples, and this form drag affects the velocity coefficient C, which is changed and is given the mean value of each experimental result.

Finally, the stability condition of the calculus of finite difference used is presumably expressed by eq. (36) sufficiently because the factor of $(\partial^2 \tilde{Z}/\partial x^2)$ in eq. (23), K', become $K'=K_0(3-\epsilon \gamma_0 \tilde{B}^{2/3} \tilde{I}_e^{-2/3})/\tilde{B}$ for $m=1$, which proves $K'=3K_0$ at the largest while the sufficient stability condition is $\Delta t/(\Delta x)^2 < K'/2$ if K' is a constant. Therefore, finite differences Δt and Δx are selected to fulfill the eq. (36).

$$\Delta t/(\Delta x)^2 < 3/2K_0 \quad\cdots\cdots\cdots\cdots\cdots\cdots\cdots\cdots\cdots\cdots\cdots\cdots\cdots\cdots\cdots\cdots\cdots\cdots\cdots\cdots\cdots(36)$$

3.3 Results of the analysis

Results of the analysis are stated, being classified into three groups, that is, the cases under simple conditions with the sand supply, ditto without the sand supply and the cases wherein some particular conditions have been added.

  (1) The cases of the initial prismatic channels with constant discharge and sand supply

The computed stream width and the bed profile are compared with the observed ones in Exp. XI and Exp. XII of large scale experiments in **Fig. 14(a)**, **(b)**
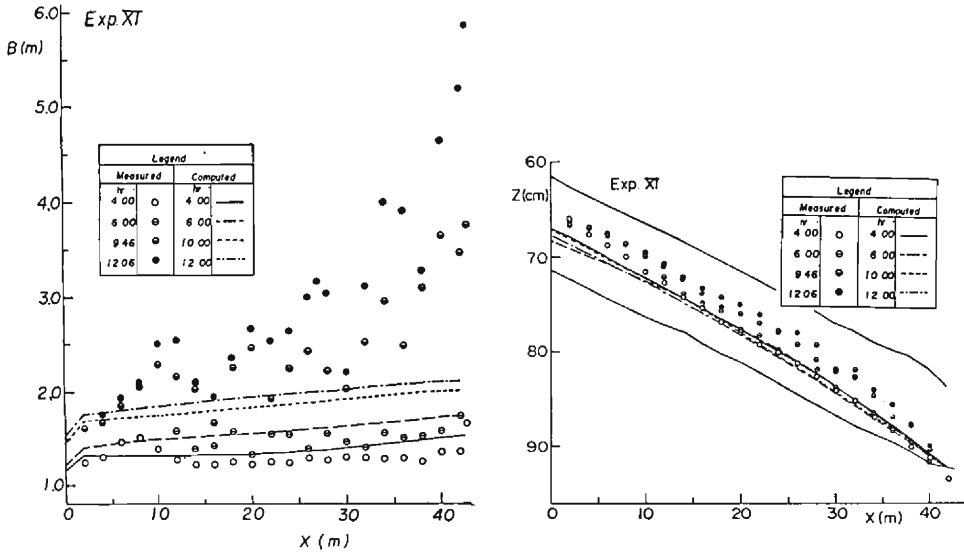

Fig. 14   The computed change of the stream width (a) and the bed profile (b) in comarison with the observed ones in Exp. XI.

and **Fig. 15(a)**, **(b)** respectively, and **Fig. 16** and **Fig. 17** are the same comparisons of stream width about Run S-3 and Run S-6 respectively.

In Exp. XI (**Fig. 14**), the computed values of the stream width and the bed elevation are quite consistent with the experimental values, showing gradually increasing tendencies of the width and uniformly large deposition in the upstream
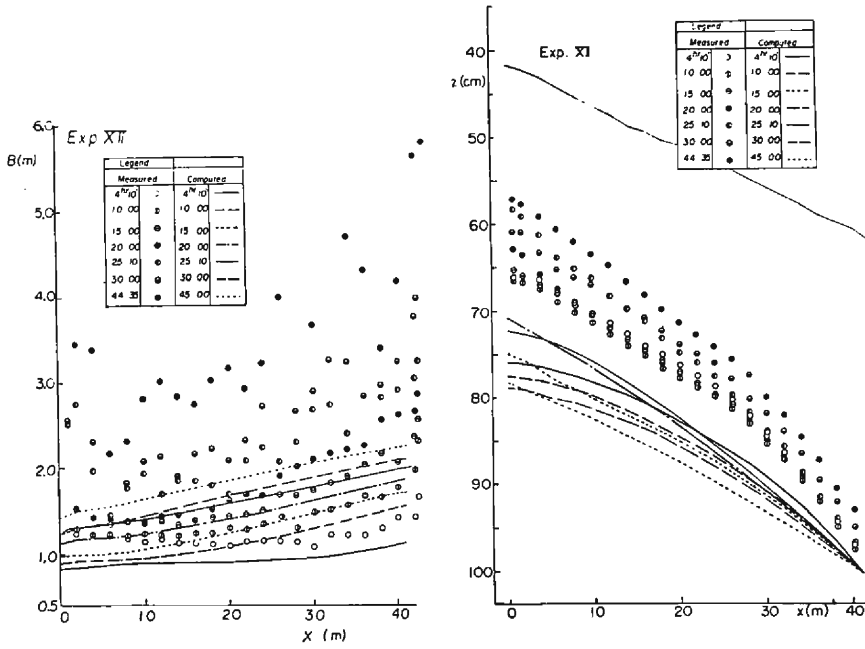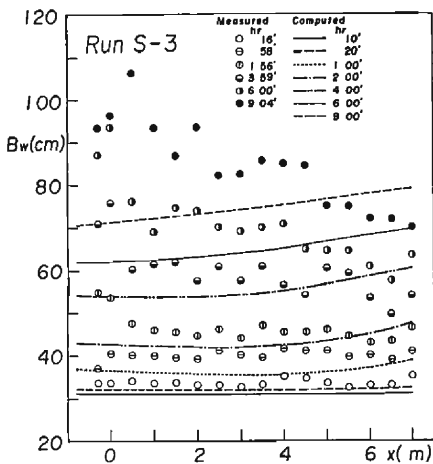

Fig. 15   The computed change of the stream width (a) and the bed profile (b) in comarison with the observed ones in Exp. XII.

Fig. 16   The computed change of the stream width and observed one in Run S-3.
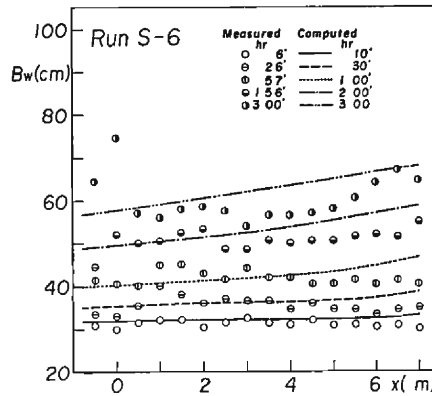
Fig. 17   The computed change of the stream width and observed one in Run S-6.

reach at the early stage and steep slope in the downstream till $T=6^{hr}$, where T is the flow duration time. After $T=6^{hr}$, the stream channel began to meander according to the development of alternating bars, and therefore the agreement turns worse. However, the smallest values of stream width of this meandering channel at the crossing section agree fairly well with the computed ones, and it seems that the final width of straight channels in the process of meandering channel formation can be predicted from this analysis.

Similarly, in Run S-3 (**Fig. 16**), consistency of stream width changes is good till $T=5^{hr}$ when the stream width reached the twice the initial one. After this, however, the injected sand was apt to deposit in the center of the stream channel because of the large width and local bank erosion is promoted by the divided flow toward both side banks. But at the midstream and the downstream reach influenced only a little by this disturbance due to sand injecting, the computed changes conform with those in the experiment. Accordingly, in spite of larger tractive force and higher sand feeding rate in Run S-6 (**Fig. 17**), the calculated values agree vrey well with the observed ones because prudent care was payed to make the rate of supply laterally uniform.

In Exp. XII (**Fig. 15**), the computed tendencies for stream width change and the bed variation conform with those of the analytical results, demonstrating the uniform widening and large aggradation in the upstream reach at the early stages. However, the agreement turns worse as the rates of channel widening and bed aggradation became much larger in the experiment than in the analysis. This discrepancy is ascribed to the fact that the analysis does not take the following process in the experiment into account. Because of the large bank height of 40 cm compared with the bottom width of 50 cm and steep slope of side bank of more than 60° of initial channel geometry, unstable banks collapsed to cause a great amount of bed aggradation and channel widening just after the beginning of the experiment, and the bed rose about 15 cm in the upstream and midstream reach, making the bed slope in the downstream reach steeper than 1/100. Furthermore, the channel widening is promoted by both the decrease in bank height corresponding to the bed aggradation and the increase in tractive force caused by the slope steepening. Therefore, the accuracy of the analysis is expected to be improved if the bank erosion formula includes the bank collapse independent of the tractive force on the elucidation of the bank erosion process.

The results of the analysis above-mentioned indicate that the one-dimensional analysis can be applied to the widening process of the straight channel which has neither local bank erosion caused by the developed alternating bars or deviation of sand feeding, nor conspicuous bank collapse not owing to the tractive force, and that the upstream boundary condition assumed before is valid in the case with sand supply.

    (2)   The cases of initial prismatic channel with constant discharge and no sand
          supply

The results of the analysis applied to Exp. II, Exp. IV and Exp. VIII are shown in
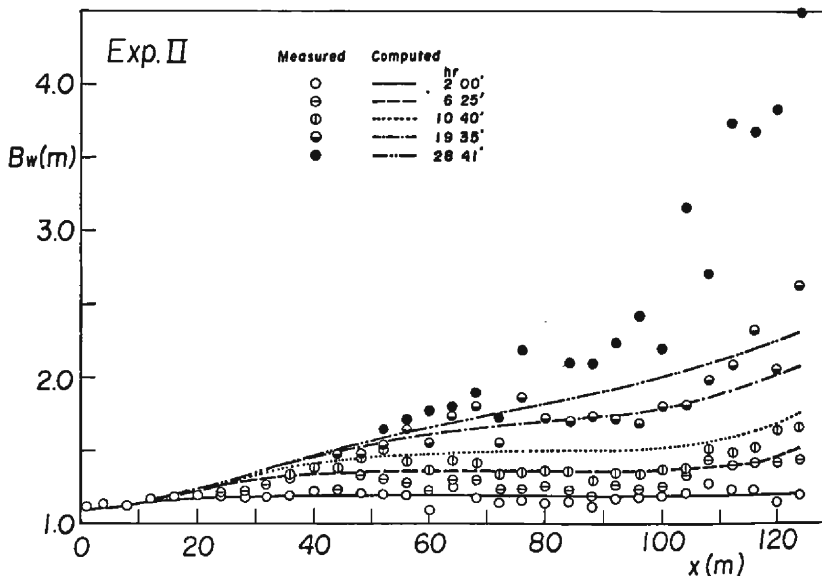
Fig. 18   The computed change of the stream width and observed one in Exp. II.

reference to the changes of stream width in **Fig. 18** to **Fig. 20**, respectively.

In these cases, all of the calculated changes have common specific aspects which are the same as the experimental ones before the development of meander: the changes of stream width divide the channel into three reaches. In upstream reach, the widening rate is low and diminishes upstream-ward corresponding to the decrease in the bed slope. In the midstream reach, the uniform widening continues till the boundary conditions are propagated from both stream ends. In the downstream reach, the widening rates are high and increase in the downstream direction according to the increase in the bed slope due to the constant bed level at the downstream end.

Especially in Exp. VIII (**Fig. 20**), the computed values agree well with the experimental ones till the final state though the widening rates in the experiment fluctuate a little due to inevitable experimental errors. In Exp. II (**Fig. 18**) and Exp. IV (**Fig. 19**), the calculated values are quite consistent with the measured ones till the channel meandering became remarkable.

Thus, the analysis proves to be applicable in these cases also and to have the limits of application due to the commencement of the channel meandering. However, it is noticeable in Exp. IV that the agreement became worse even in an $x=0$–70 m reach where channel meandering did not progess remarkably. Two reasons can be considered for this disagreement separately: that at $x=0$–20 m reach where the computed values exceed the measured ones, and that at $x=30$–60 m reach where the inverse occurred.

It is supposed as a reason for the former that the upstream boundary condition of

the static equilibrium bed slope and subsequent constant width was not satisfied immediately after the beginning of the experiment. This is assured by a result of the analysis applied to Run S-5, in which the stream reach was short and the boundary conditions were dominant in the whole reach. Furthermoer, the difference between
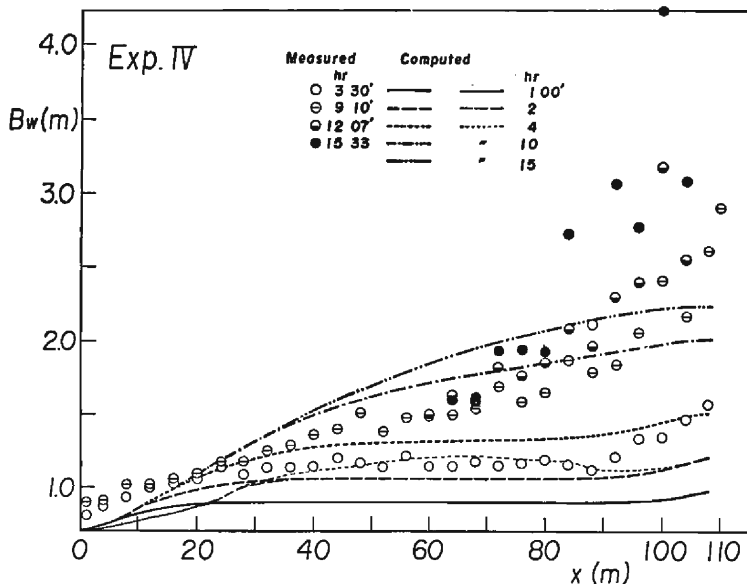

Fig. 19   The computed change of the stream width and observed one in Exp. IV
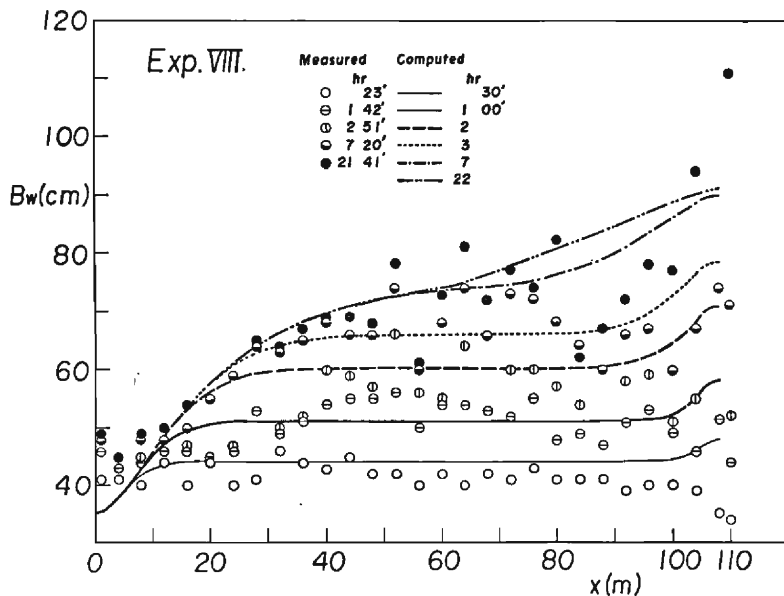(fine lines are the results computed with eq. (37)).

Fig. 20   The computed change of the stream width and observed one in Exp. VIII

the computed values and the measured ones is more conspicuous in the upstream reach while being indiscernible in the downstream reach. By constrast, in the case where the length of the stream reach is excessively large compared with dimensions of the cross section, such as in Exp. VIII of 110 m in length to 0.25 m in width, the reach influenced by the boundary condition at the upstream end become less noticeable. Besides, the reach influenced by hte boundary condition at the upstream end seems to be much shorter in Exp. II than in others.

In Exp. II and Exp. IV, only the initial cross sectional dimensions differ from each other, that is, $B_0 = 1.1$ m and $D = 0.2$ m in Exp. II, while $B_0 = 0.7$ m and $D = 0.1$ m in Exp. IV, hence tractive force in Exp. IV became larger than that in Exp. II in the early stage. Accordingly, the reach involved in this disagreement is presumed to be elongated when the difference of the tractive force becomes large between that actually appearing and that estimated from eq. (35) in the upstream reach corresponding to the most upstream finite difference. Though the propagation of this boundary condition relates to the finite difference, especially that of distance, considering that eq. (35) is a specific form of eq. (34) reduced from the relation of sediment transport in an equilibrium state, these equations are more or less incomplete for the boundary condition at the upstream end where the sediment transport has a rather intense property of non-equilibrium. Therefore, if a bed slope estimated by these euqations resembles the initial one, which may be the cases of Exp. II and the experiments mentioned in the subsection (1), they become a good approximation, while if a difference between these slopes is large the other boundary condition must be established on the consideration of the mechanism of seidment transport at the upstream end.

Next, the occurrence of the reach where the computed width becomes greater than the measured one is ascribed to the simple assumption of the bank erosion process by use of eq. (19) into which the effects of the variation of water stage and of the armouring phenomenon near the bank are not introduced. According to the results of the experimental observation, the lowering of water stage or bed level has an apparent tendency to restrain the side bank erosion, particularly in the experiments of large-scale with a fairly wide distribution of grain size. Actually, this type of reach obviously appeared in order of Exp. IV, Exp. II and Exp. VIII. The bed degradation was conspicuous in the same order. However, executing the analysis into which these effects were introduced as a simple additional expression below,

$$\Delta B / \Delta t = 0 \qquad \text{for} \qquad \Delta z / \Delta t \leq 0 \tag{37}$$

the results indicated that the condition above gives a more strict restraint than the observation as shown in **Fig. 19** by fine lines about Exp. IV. The effect of the bed degradation on the bank erosion process requires the consideration based on the phenomena occuring on the slope of the side bank, the same as the case of the bank collapse.

(3) The cases with additional specific conditions

In this subsection, the results of the analysis applied to three cases with additional specific conditions are stated: The cases are the experiment with an initial slope of two-steps, Exp. VI; that under varying step-like discharge, Exp. VII; and that with a rigid right side bank, Exp. IX.

As for Exp. VI, there was a somewhat inadequate condition of the conjunction between the upstream reach and the downstream one at the transition point of slope in a previous analysis[4], hence the x-axis is taken along the bottom center line of the initial bed in the upstream and is used in common for the downstream reach. The initial bed profile is given as a linear function of distance x in this reach. **Fig. 21** demonstrates the results about the stream width of the analysis executed under the initial condition above. The computed values agree well with observed ones even
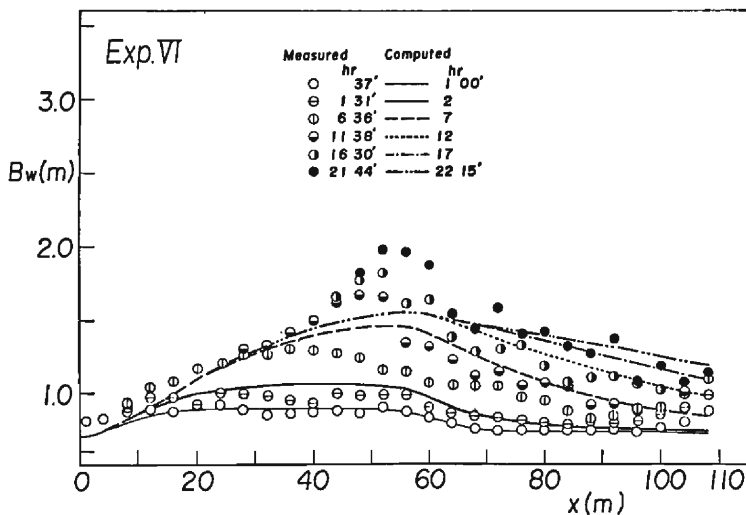
Fig. 21 The computed change of the stream width and observed one in Exp. VI.

in the reach near the conjunction point, showing a higher rate of widening in the upstream raech than in the downstream one in accordance with the initial bed slope and the inverse tendency with approach to the final stage till $T=22^{hr}$ after which channel meandering became remarkable, though the computed values have a little higher rate of channel widening than the observed ones.

The analysis for Exp. VII was carried out, starting from the initial geometry and regarding a final state of the stream channel at a preceding stage of discharge as an initial condition for the following stage, and the analysis was ended when the channel widening stopped throughout the whole reach during the recession stage. The results of the analysis concerning the stream width are compared with the experimental values in **Fig. 22**. The calculated values show a good agreement in both longitudinal variation and the change with time at the midstream and downstream reach, though
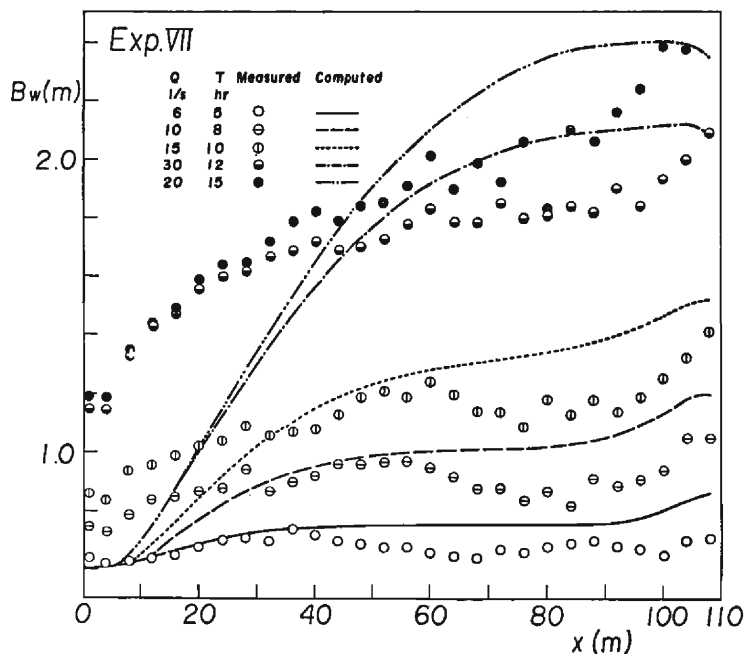
Fig. 22   The computed change of the stream width and observed one in Exp. VII.
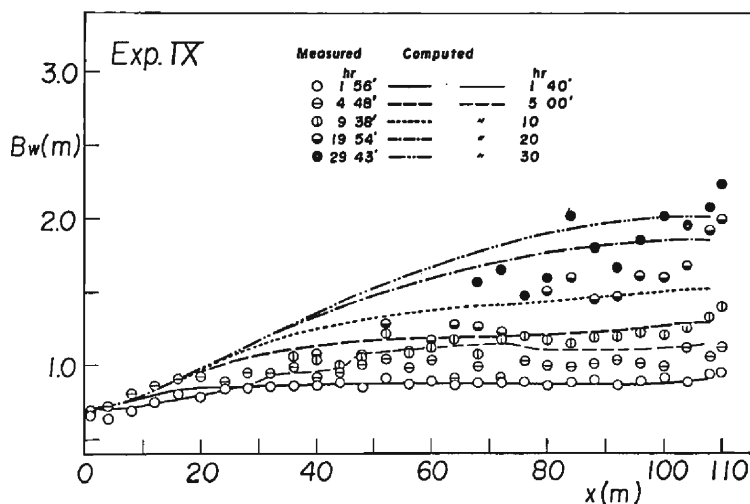(fine lines are the results computed with eq. (37)).

Fig. 23   The computed change of the stream width and observed one in Exp. IX.
(fine lines are the results computed with eq. (37))

experimental error must be taken into account.   However, the disagreement due to
the incompleteness of the boundary condition occurs in the upstream reach except
for a stage of small discharge of $Q=6$ l/sec, and the length of this reach becomes
large in accordance with the increase in the discharge because of the reason mentioned

before. It is conlcuded that the accuracy of the analysis is fairly sufficient for the case under the varying flow condition and will be improved if the suitable boundary condition is given at the upstream end.

Finally, in the case of Exp. IX, the widening process is computed with a value of the coefficient in the bank erosion formula N_1 half the value of the other cases since the bank erosion occurred only at the left side bank. The computed changes of the stream width are depicted in **Fig. 23** along with measured ones. In the experiment the bed degradation was propagated rapidly from upstream end because of little sand supply due to the bank erosion, and the stabilizing effect according to the bed degradation is remarkable enough to stop the channel widening in $x=0$–60 m reach by $T=10^{\mathrm{hr}}$. Since the bank erosion formula does not include this effect as stated before, the computed width becomes larger than the observed one and the agreement turns bad after $T=2^{\mathrm{hr}}$ in the whole reach. But the conformity of the calculated changes with the measured ones is improved remarkably in the result of the analysis into which eq. (37) is introduced, as demonstrated by a fine dashed line in **Fig. 23**. Thus, in case of the experimental process accompanied by extreme bed degradation, the condition expressed by eq. (37) proves to compensate well the insufficiency of the bank erosion formula. In addition, a rapid increase in the stream width at $x=70$–100 m reach after $T=10^{\mathrm{hr}}$ is caused by migratory local erosion of the loose bank due to alternating bars formed in this reach. It seems that the one-dimensional analysis can be applied to the widening process in the stream channel with a rigid bank on one side.

Being based on these results mentioned in above subsections, the one-dimensional analysis of stream channel variation has high applicability for the prediction of the widening process in the straight channel where bars have not developed enough to cause the local bank erosion, in spite of several simplifications. For the promotion of accuracy of this analysis, the following two points need to be elucidated. One of them is the clarification of the boundary condition at the upstream end in the case of the large difference between the ability of the initial sediment transport and the sediment supply rate; the other is the introduction of the bank erosion formula including the conditions of the bank collapse and the stabilizing effect caused by the lowering of the bed or the water level. The alternating bar's behavior is, needless to say, another important factor in the channel widening process and, in fact, give the limit of the application of this one-dimensional analysis.

4. Conclusion

On the widening process of straight stream channels, which is the most fundamental and the simplest fluvial process in alluvial rivers, the significance of its investigation and the outline of previous studies have been stated first. Next, the movement path of the sand eroded from the side bank and the variation process of cross sectional shape were considered by carrying out detailed experiments. Finally,

the validity of the one dimensional analysis of stream channel variation is clarified under various initial and hydraulic conditions. The results obtained in this study are summarized in the following as the concluding remarks.

As the results of the tracer test by use of colored sand on the movement path of the sand eroded from side banks, it has been determined that most of the collapsed sand deposits on the stream bed passing through the side slope near the water's edge, and that the influence of the bank collapse on the transporting direction becomes indiscernible in a certain distance from the water's edge.

From the cross sectional changes of a stream channel, the lateral component of sediment load is estimated in the early stage with little longitudinal variation by computing the sediment balance. This lateral component yields an approximate expression of the direction of sediment movement, being divided by the longitudinal one evaluated from the Brown type bed load function. Furthermore, the process of the cross sectional change is simulated by use of this approximate expression. The dealing with slopes steeper than the angle of repose appearing in the execution of the analysis and the boundary condition at the water's edge are pointed out as major problems of this simulation.

On the other hand, as to the channel widening process under longitudinally varying conditions, the fundamental equations of the one-dimensional analysis of stream channel variation are described with consideration of the initial and boundary conditions. Its high applicability is clarified under various hydraulic ocnditions classified into three groups: the cases of initial prismatic channels with constant discharge and sand supplying; ditto except for no sand supplying; and the cases otherwise where some particular conditions were added to the initial stream channel or the discharge. It is concluded that the widening process of the straight stream channel can be predicted by the extended one-dimensional analysis till the beginning of remarkable stream meandering mainly caused by well-developed alternating bars. However, the applicability turns worse when a remarkable bed aggradation is caused by the collapse of side banks and when a large difference exists between the initial ability of sediment transport and the sand supplying rate.

In order to extend the applicability of the analysis to these cases, the side bank erosion process has been investigated based on hydrodynamic equations, including the collapse of side bank and the effects of the water stage variation[9], and the non-equilibrium property of the sediment transport at the upstream end is considered on the continuity relation of the volumetric change in a certain reach near the end such as that corresponding to the first finite difference.

Acknowledgement

References

1) Hasegawa, K., K. Kudo and I. Yamaoka: An Experiment of Stream Channel Meandering, Proc., 23rd Annual Scien. Lect. Meeting, JSCE, 1968, pp. 385–388 (in Japanese).

2) Adachi, S. and T. Nakato: Experiments on Channel Widening of Alluvial Streams, Proc. 24th Annual Scien. Lect. Meeting, JSCE, 1969, pp. 253–254 (in Japanese).

3) Tsubaki, T., M. Hirano and K. Tanaka: Process of Stream Channel Variation with Bank Erosion, Proc., 15th Japanese Conf. on Hydraulics, Hydraulic Committee of JSCE, 1971, pp. 43–48 (in Japanese).

4) Ashida, K., Y. Muramoto and S. Narai: Studies on Fluvial Processes of Stream Channels (2)— Self-formed Stable Channle Profile and Process—, Annuals, Disast. Prev. Res. Inst., Kyoto Univ., No.-14B, 1971, pp. 265–297 (in Japanese).

5) Hirano, M.: River-bed Variation with Bank Erosion, Proc., JSCE, No. 210, 1973, pp. 13–20 (in Japanese).

6) Muramoto, Y., S. Tanaka and Y. Fujita: Studies on Fluvial Processes of Stream Channels (3)— One-dimensional Analysis of Channel Process and Characteristics of Self-formed Meandering Channels—, Annuals, Disast. Prev. Res. Inst., Kyoto Univ., No. 15B, 1972, pp. 385–404 (in Japanese).

7) Hasegawa, K.: Bank-erosion Discharge Based on a Non-equilibrium Theory, Proc., JSCE, No. 316, 1981, pp. 37–50 (in Japanese).

8) Ashida, K. and M. Michiue: Study on Hydraulic Resistance and Bedload Transport Rate in Alluvial Streams, Proc., JSCE, No. 206, 1972, pp. 59–69 (in Japanese).

9) Fujita, Y.: Studies on Stream Channel Processes in Alluvial Rivers, Doctral Thesis, Kyoto Univ., 1981, pp. 63–81 (in Japanese).

10) Lane, E.W.: Design of Stable Channels, ASCE Transactions, Vol. 120, Paper No. 2776, 1955. pp. 1234–1279.

11) Fujita, Y. and Y. Muramoto: Experimental Study on Stream Channel Processes in Alluvial Rivers, Bull., Disast. Prev. Res. Inst., Kyoto Univ., Vol. 32, Part 1, No. 288, 1982, pp. 49–96.